Magazine of Civil Engineering

ISSN 2712-8172

journal homepage: http://engstroy.spbstu.ru/

Research article

UDC 614.844.5:614.844.2

DOI: 10.34910/MCE.131.2

Mathematical model of foam expansion rate generated in sprinklers

A.N. Kamluk , ***A.O. Likhomanov*** ✉ , ***E.G. Govor*** , ***A.V. Grachulin***

University of Civil Protection of the Ministry of Emergency Situations of the Republic of Belarus, Minsk, Republic of Belarus

✉ *alexlikh20@gmail.com*

Keywords: automatic foam extinguishing system, sprinkler, nozzle, foam, foam expansion, fluid dynamics

Abstract. Foam solution discharge is always accompanied by changes in the operating pressure due to different pressure losses along the pipeline in automatic foam extinguishing systems. Changes in the operating pressure affect the process of a liquid jet fragmentation into droplets and the formation of foam films. Therefore, to increase the accuracy of calculations when designing automatic foam extinguishing systems, it is worthwhile to evaluate the main characteristics of the foam in terms of fire extinguishing efficiency, in particular, its expansion. For this purpose, the generalization of the experimental data using the theory of similarity and taking into consideration the hydrodynamic features of the deflector type sprinkler operation and the properties of foam solution was carried out to develop a novel simplified mathematical model. This model allows to predict the foam expansion depending on the geometric parameters of the sprinkler elements and the empirical coefficient, which takes into account the peculiarities of the chemical composition of the foam concentrate. This new model predictions of foam expansion show good agreement with the experimentally measured foam expansion. The average error in foam expansion was less than 9 %.

Citation: Kamluk, A.N., Likhomanov, A.O., Govor, E.G., Grachulin, A.V. Mathematical model of foam expansion rate generated in sprinklers. Magazine of Civil Engineering. 2024. 17(7). Article no. 13102. DOI: 10.34910/MCE.131.2

1. Introduction

The object of current research is air-mechanical foam, which is used to extinguish fires in automatic foam extinguishing systems (AFES). The AFES are one of the main parts of fire protection systems for chemical, oil refining, metallurgical, and energy enterprises[1] [1–3]. The AFES are intended to automatically discharge the extinguishing agent without human involvement to the protected area to localize or eliminate fire at the initial stage with minimal damage, as well as to prevent re-ignition of the combustible substance by creating the foam cushion. Air-mechanical foam, which is used as fire extinguishing agent in the AFES, is the aggregate of air-filled bubbles formed by mechanical mixing an aqueous solution of a suitable foam concentrate and air in the foam sprinklers and foam generators. One of the main classification characteristics of air-mechanical foam in terms of fire extinguishing efficiency is its expansion. Foam expansion is a ratio of the volume of foam to the volume of the foam solution from which it was made [4, 5]. Foam is usually classified into three main groups based on the conditions of application (extinguishing method, type of combustible material, type of foam concentrate, etc.): low-expansion (with expansion in the

[1] McGree, T. U.S. Experience with Sprinklers [Online]. URL: https://www.nfpa.org/News-and-Research/Data-research-and-tools/Suppression/US-Experience-with-Sprinklers (date of application: 01.07.2024).

range from 1 to 20), medium-expansion (with expansion in the range from 21 to 200), and high-expansion (with expansion greater than 200) [5, 6]. Low-expansion foam is intended mainly for putting out fire over its entire area. Such foam has greater penetration ability, better spreads on the protected area, and cools burning surfaces more effectively than other types of foam [7, 8]. It is common knowledge that the higher the expansion of foam (in the range from 1 to 20), the greater its extinguishing efficiency would be [4, 9].

In the AFES, low-expansion foam is usually generated using deflector type sprinklers [6]. Foam solution discharge is always accompanied by changes in the operating pressure due to different pressure losses along the pipeline. Changes in the operating pressure affect the process of a liquid jet fragmentation into droplets and the formation of foam films [10, 11]. Therefore, to increase the accuracy of calculations when designing the AFES, it is worthwhile to evaluate the main characteristics of foam in terms of fire extinguishing efficiency, in particular, its expansion. In this case, both the geometry of the sprinkler and the hydrodynamics of foam solution flow must be taken into consideration.

Previous studies of the influence of sprinkler geometry were associated, as a rule, with optimizing the water flux distribution and uniformity, which is formed by the fire sprinkler head. In [12], the author tried to resolve the initial spray structure of fire sprinklers with a volume-of-fluid modeling. He studied the initial spray formation process of commercial fire sprinklers with a large-eddy simulation and a volume-of-fluid model. Then he determined factors affecting water flux distribution of fire sprinklers and effect of water flux uniformity on fire suppression characteristics and optimized the fire sprinkler head design using a micro-genetic algorithm to produce a uniform distribution of droplet size and water flux [13, 14]. The final optimized design showed that the section angle of the fire sprinkler head should be larger, the tines should be more protruding, and the slots should be more concave to improve the water flux distribution. However, the author noted that caution should be exercised when applying these results to conditions other than those used in this study.

Previously, many studies were carried out to develop models for predicting the distribution of water flux and quite accurate and adequate models were obtained [15–19]. However, all studies carried out to date by other authors have focused on water. Foam is a dispersed system with a gas dispersed phase and a liquid dispersion medium. The water and foam spray simulations differ significantly from each other. To predict the expansion of foam, we have studied its dependence on the geometric parameters of the deflector type sprinkler in [11, 20]. As a result, we developed the regression model as a polynomial to predict the foam expansion K depending on the sprinkler frame arm length L (mm), the outer deflector diameter D (mm), the tine inclination angle α (deg), and the deflector working surface coefficient K_S (%):

$$\begin{aligned} K = {} & 50.7 - 1.012L + 0.00412L^2 - 1.117K_s + 0.00686K_s^2 - 0.129D + \\ & + 0.00077D^2 + 0.0625\alpha - 0.00087\alpha^2 + 0.02769LK_s - 0.0001715LK_s^2 - \\ & - 0.0001194L^2K_s + 0.000000747L^2K_s^2 + 0.00107LD - 0.0000067LD^2 + \\ & + 0.00073K_sD - 0.000005K_sD^2. \end{aligned} \quad (1)$$

The developed regression model has high accuracy (the coefficient of determination R^2 is equal to 0.97). This model can be successfully implemented for engineering new sprinklers for the protection of buildings and structures of different types. However, the developed model is just a regression equation, which is why it is not interpretable. The field of its application is limited by the conditions of experiments and measurements based on which it was developed. In particular, it concerns the hydrodynamic parameters of the flow of foam solution, which are governed by the geometry of the flow path of the sprinkler nozzle and the properties of the foam solution.

For this reason, the main goal of current research is to develop a simplified mathematical model with variables in a dimensionless form, which would provide a possibility to evaluate the effect of the geometric parameters of the frame arm and the deflector of the sprinkler, the hydrodynamic parameters of the jet and the properties of the foam solution on the foam expansion.

2. Methods

2.1. Hydrodynamic Parameters of the Jet

A jet is formed when liquid is delivered through a hole of some diameter into an open space. As it moves, it directly interacts with the environment. Due to the mutual action of the inertia forces, the surface tension, the viscous friction, and the aerodynamic forces, perturbations (i.e. waves) appear on the outer longitudinal boundary of the jet. The integrity of the jet brakes when the amplitude of oscillations increases

to a certain critical value. After that, the jet gets the gradual fragmentation resulting in the formation of small structures (i.e. ligaments) and droplets [21, 22].

It is known that liquid jets break up in several regimes: the laminar or turbulent Rayleigh regime, the downstream transition regime, the turbulent surface breakup regime, and the atomization regime (Fig. 1) [23]. Each of the regimes is characterized by certain combinations of the acting forces and differs from each other by the hydrodynamics and the structure of the jet if the operating parameters are changed (e.g. pressure). To summarize the experimental data, the dimensionless quantities like the Reynolds number (Re), the Weber number (We), and the Ohnesorge number (Oh) are generally used in the studies of liquid jets break up process (Fig. 2). These numbers represent the relation between the inertia forces, the viscous friction forces, and the surface tension [25]:

$$Re = (uD_h)/\nu; \quad We = \left(\rho D_h u^2\right)/\sigma_s; \quad Oh = \eta/\sqrt{\sigma_s \rho D_h}, \tag{2}$$

where u is a characteristic jet velocity, m·s^{-1}; D_h is a hydraulic diameter, m; ν is a kinematic viscosity of the foam solution, m^2·s^{-1}; η is a dynamic viscosity of the foam solution, Pa·s; σ_s is a surface tension coefficient, N·m^{-1}, and ρ is a density of the foam solution, kg·m^{-3}.

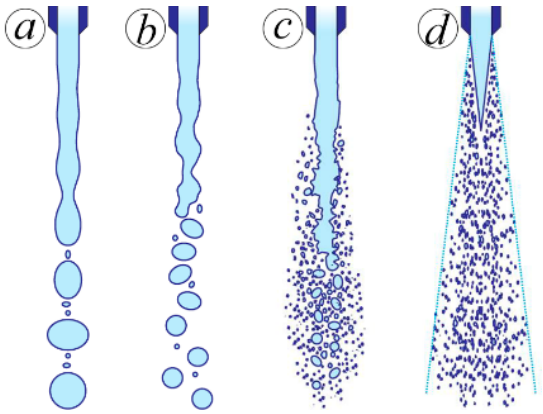

Figure 1. Schematic view of the jet breakup process regimes (*a* is the laminar Rayleigh, *b* is the downstream transition, *c* is the turbulent surface breakup, and *d* is the atomization regime) [23].

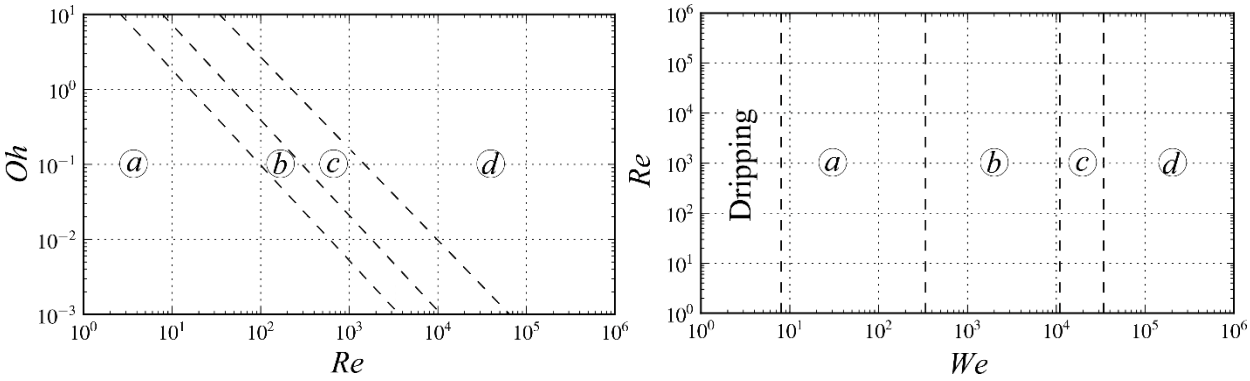

Figure 2. Diagrams that are used to determine the jet breakup process regime (*a* is the laminar Rayleigh, *b* is the downstream transition, *c* is the turbulent surface breakup, and *d* is the atomization regime) [25].

When it comes to deflector type sprinklers, the breakup process of liquid jet usually occurs in the turbulent surface breakup or atomization regimes (Fig. 2, positions c and d), since the outflow of the foaming solution occurs through the nozzle flow path of a fairly small diameter (from 8 to 25 mm) at a very high velocity (usually significantly more than 10 m/s). In that case, the inertia forces, the viscous friction forces, and aerodynamic forces have the greatest influence on the jet breakup process [24]. Taking into account the fact that the foam solution contains surfactants that change the surface tension of the liquid but do not affect its kinematic and dynamic viscosity, it is appropriate to use the Weber number to summarize the experimental data. It has been well studied that the length of waves formed on the jet surface after leaving the orifice of the sprinkle nozzle is inversely proportional to the Weber number, and their amplitude, on the contrary, is directly proportional to it [22, 26]. When the Weber number increases, a more

intense breakup process of the jet into small structures and droplets is observed. Moreover, that, in its turn, can affect the foam generation process in the sprinkler.

2.2. Foam Solution Properties

According to (2), the dimensionless quantities used to determine the physical similarity of turbulent flows include a number of variables that characterize the physical and chemical properties of the fluid, which are density, surface tension coefficient, dynamic and kinematic viscosities. Accordingly, by varying the values of these parameters, the character of fluid flow (average velocity, geometry, and structure of the jet) also changes. Working foam solutions made of commercially produced foam concentrates have almost identical physical and chemical properties, values of which fluctuate in narrow ranges under normal ambient conditions: ρ = 1000–1020 kg·m^{-3}, σ_s = 0.029–0.032 N·m^{-1}, η = (9.0–9.4)·10^{-4} Pa·s, and ν = (0.89–1.00)·10^{-6} m^2·s^{-1}. It follows that at the same operating pressure of the foam solution before the nozzle of the sprinkler with the same geometric parameters of the flow path, the character of the flow of liquid before not reaching the frame arm and the deflector of the sprinkler is generally identical despite the use of different types and brands of foam concentrates. Nevertheless, foam expansion actually differs for various types and brands of foam concentrates if geometrically identical sprinklers are used as it was shown in the experimental study [27]. Therefore, one can assume that the foam expansion depends on the chemical composition of the foam concentrate and, consequently, on the type and nature of the chemical reactions occurring during the foam generation process. It should be noted that the influence of the nature of reagents in the composition of modern foam concentrates, as well as their concentration in the working foam solution on the parameters of the foam generation process is poorly studied. In particular, it is due to the lack of data on the chemical composition of the foam concentrates on the market.

To take into consideration composition peculiarities of foam concentrate in the simplified mathematical model for the determining foam expansion, an empirical coefficient $\gamma_{e.r}$ can be implemented. This coefficient can be determined experimentally and calculated as a ratio of the foam expansion for the foam concentrate under study $\left(K_{e.r}\right)$ to the foam expansion for some reference foam concentrate $\left(K_{st}\right)$. For example, on the territory of the Republic of Belarus, one of the most popular foam concentrate of type S (in sense that it is a synthetic hydrocarbon foam concentrate without fluorinated surfactants) is PO-6RZ (“ПО-6РЗ” in Russian). Therefore, in our study, we implemented PO-6RZ as the reference foam concentrate. The coefficient $\gamma_{e.r}$ is assigned a value of 1 for it.

In [27], the experimental determining of the main characteristics of foam, in particular its expansion, was carried out using 13 deflector type sprinklers with different geometric parameters of its elements and 3 different foam concentrates. After some straightforward transformations of the experimental data obtained in [27], we plotted the dependences of the foam expansion for type S foam concentrate Syntek-6NS (“Синтек-6НС” in Russian) and type WA foam concentrate OPS-0.4 (“ОПС-0.4” in Russian) on the foam expansion for the reference foam concentrate PO-6RZ (Fig. 3). As it follows from Fig. 3, the dependences are linear. It allow us to determine the values of the coefficient $\gamma_{e.r}$ for the foam concentrates under study: 0.92 for Syntek-6NS and 0.68 for OPS-0.4, respectively.

It must be emphasized that in the previous studies [11, 20, 25, 27], an aqueous solution with the manufacturer's recommended concentration of the foam concentrate in it (6% for PO-6RZ and Syntek-6NS, 1 % for OPS-0.4) was used.

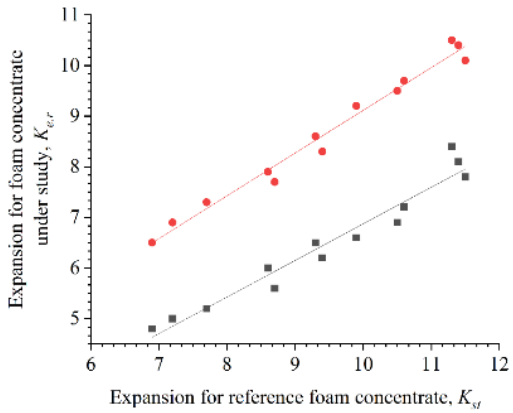

Figure 3. The dependence of foam expansion for foam concentrates Syntek-6NS (circles) and OPS-0.4 (squares) on foam expansion for the reference foam concentrate PO-6RZ (based on [27]).

2.3. Geometric Parameters of the Sprinkler

Geometric parameters of the elements of the deflector type sprinkler are presented in Fig. 4.

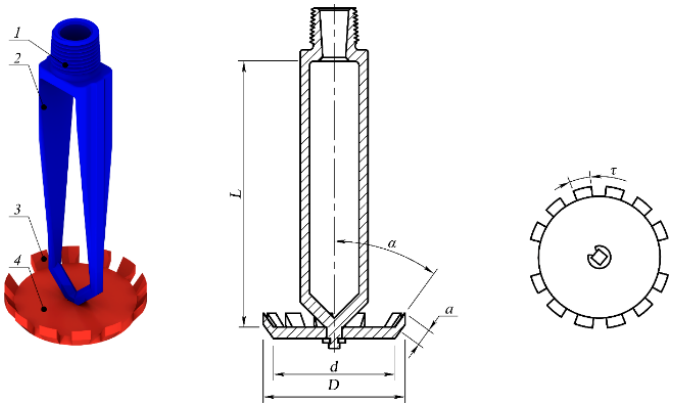

Figure 4. Main elements of the deflector type sprinkler and its geometric parameters (*1* is the nozzle; *2* is the frame arm; *3* is the tine; *4* is the deflector; D is the outer deflector diameter; a is the tine length; d is the inner deflector diameter; τ is the deflector tine spacing angle; α is the tine inclination angle; L is the frame arm length) [27].

To account for individual geometric parameters, such as the inner deflector diameter d and the deflector tine spacing angle τ, the deflector working surface coefficient K_s is used [27]:

$$K_s = \frac{360d^2 \sin\alpha + \left(D^2 - d^2\right)\sum\tau}{360\left(d^2 \sin\alpha + D^2 - d^2\right)} \cdot 100\% = \\ = \frac{360d^2 \sin\alpha + \left(\left[d + \left(D_y - d\right)\sin\alpha\right]^2 - d^2\right)\sum\tau}{360\left(d^2 \sin\alpha + \left[d + \left(D_y - d\right)\sin\alpha\right]^2 - d^2\right)} \cdot 100\%, \quad (3)$$

where $D_y = d + 2a.$

To make a decision about the geometric parameters of the sprinkler frame arm and deflector for inclusion in a simplified mathematical model, the results of the dispersion analysis of experimental data obtained in [28] (Fig. 5) were used. As seen in Fig. 5a, among the individual factors (the first 8 rows of the table), the deflector working surface coefficient K_s ("Coefficient $K_s(\mathrm{L})$") characterizes most of the variability of foam expansion (the sum of squares of deviations "SS" is equal to 19.56, which is about 27 % of the total sum of squares of deviations "Total SS"). The deflector working surface coefficient K_s is followed by the frame arm length ("Length $L(\mathrm{L})$" and "Length $L(\mathrm{Q})$" in Fig. 5a), the outer deflector diameter ("Diameter $D(\mathrm{L})$" and "Diameter $D(\mathrm{Q})$" in Fig. 5a), and the tine inclination angle ("Inclination $\alpha(\mathrm{L})$" and "Inclination $\alpha(\mathrm{Q})$" in Fig. 5a) when it comes to influence on the foam expansion. It should be noted that the tine inclination angle α describes a very small part of the variability of the foam expansion (2 % of the total sum of squares of deviations). In addition, according to the table of factor effects estimation in Fig. 5b, the tine inclination angle practically does not affect the value of the foam expansion (ΔK is no more than 0.3). Therefore, this factor can be neglected.

a)

Factor	ANOVA; Var.:Expansion *K*; R-sqr=,97145; 4 3-level factors, 1 Blocks, 81 Runs; DV: Expansion *K* SS	df	MS	F	p
(1) Length L(L)	5,47157	1	5,47157	169,3029	0,000000
Length L(Q)	7,13405	1	7,13405	220,7439	0,000000
(2) Coefficient K_s(L)	19,56444	1	19,56444	605,3686	0,000000
Coefficient K_s(Q)	0,15635	1	0,15635	4,8380	0,031459
(3) Diameter D(L)	2,61717	1	2,61717	80,9812	0,000000
Diameter D(Q)	2,14352	1	2,14352	66,3254	0,000000
(4) Inclination α(L)	1,23005	1	1,23005	38,0604	0,000000
Inclination α(Q)	0,69751	1	0,69751	21,5826	0,000017
1L by 2L	15,47111	1	15,47111	478,7116	0,000000
1L by 2Q	5,50298	1	5,50298	170,2747	0,000000
1Q by 2L	0,25411	1	0,25411	7,8627	0,006673
1Q by 2Q	0,73069	1	0,73069	22,6091	0,000012
1L by 3L	16,38001	1	16,38001	506,8350	0,000000
1L by 3Q	4,96141	1	4,96141	153,5173	0,000000
2L by 3L	0,26488	1	0,26488	8,1959	0,005669
2L by 3Q	0,42603	1	0,42603	13,1823	0,000563
Error	2,06837	64	0,03232		
Total SS	72,44401	80			

b)

Factor	Effect Estimates; Var.:Expansion *K*; R-sqr=,97145; 4 3-level factors, 1 Blocks, 81 Runs; MS Residual=,0323182 DV: Expansion *K* Effect	Std.Err.	t(64)	p	-95,% Cnf.Limt	+95,% Cnf.Limt
Mean/Interc.	8,732330	0,021422	407,6324	0,000000	8,689534	8,775125
(1) Length L(L)	0,658253	0,050590	13,0116	0,000000	0,557189	0,759317
Length L(Q)	0,694519	0,046745	14,8575	0,000000	0,601134	0,787903
(2) Coefficient K_s(L)	1,253015	0,050927	24,6042	0,000000	1,151277	1,354753
Coefficient K_s(Q)	0,102222	0,046474	2,1995	0,031459	0,009379	0,195065
(3) Diameter D(L)	-0,465572	0,051736	-8,9990	0,000000	-0,568927	-0,362217
Diameter D(Q)	0,368674	0,045269	8,1440	0,000000	0,278239	0,459110
(4) Inclination α(L)	0,301852	0,048928	6,1693	0,000000	0,204107	0,399597
Inclination α(Q)	0,196852	0,042373	4,6457	0,000017	0,112202	0,281501
1L by 2L	1,311111	0,059924	21,8795	0,000000	1,191399	1,430824
1L by 2Q	0,716667	0,054921	13,0489	0,000000	0,606948	0,826385
1Q by 2L	0,155926	0,055607	2,8041	0,006673	0,044837	0,267014
1Q by 2Q	0,242333	0,050965	4,7549	0,000012	0,140519	0,344148
1L by 3L	1,259032	0,055925	22,5130	0,000000	1,147310	1,370755
1L by 3Q	0,606304	0,048934	12,3902	0,000000	0,508547	0,704061
2L by 3L	0,162103	0,056623	2,8628	0,005669	0,048986	0,275221
2L by 3Q	0,179886	0,049545	3,6307	0,000563	0,080908	0,278864

Figure 5. ANOVA analysis of variance (*a*) and estimation of factor effects (*b*) carried out using STATISTICA software (SS is the sum of squares of deviations, df is the number of degrees of freedom, MS is the mean squares of deviations (MS = SS/df), F is the *F*-test (MSfactor/MSerror), p is the statistical significance level (*p*-value), Error is the error of the experiment, Total SS is the total sum of squares of deviations) [28].

Thus, the simplified mathematical model for determining the foam expansion can be represented in dimensionless form as follows:

$$K = B_e \gamma_{e.r} K_s^c \left(L/D\right)^g \left(D/D_{\max}\right)^q We^z, \quad (4)$$

where B_e is the empirical coefficient; c, g, q, z are the powers of the equation variables; $D_{\max}$ is the largest diameter of the sprinkler deflector and equal to 100 mm. The dimensionless parameter $\left(L/D\right)$ represents the relative length of the sprinkler frame arm, and the $\left(D/D_{\max}\right)$ is the scaling factor.

3. Results and Discussion

The search for the values of c, g, q, and z from (4) was performed by taking the natural logarithm of this equation and comparing it with the obtained experimental dependences of the foam expansion K on the included variables. The values of powers are taken equal to the slope of regression lines for the corresponding dependencies. For the dependences $\ln\left(K\right) = f\left(\ln\left(K_s\right)\right)$ and $\ln\left(K\right) = f\left(\ln\left(D/D_{\max}\right)\right)$, the slopes are: c = 0.5 and q = –0.05 (Fig. 6, 7). The dependence

$\ln(K) = f(\ln(L/D))$ is non-linear and the regression line is a curve with a maximum in the range L/D = 3.0 ± 0.3 (Fig. 8). For this reason, we decided to divide the dependence $\ln(K) = f(\ln(L/D))$ into two linear sections with slope coefficient g equal to 0.10 at L/D ≤ 3.0 (Fig. 8, position 1) and –0.03 at 3.0 < L/D ≤ 7.5 (Fig. 8, position 2).

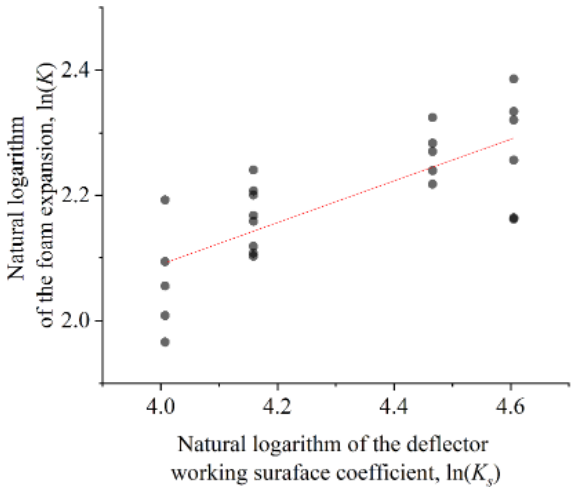

Figure 6. Dependence of the natural logarithms of the foam expansion and the deflector working surface coefficient.

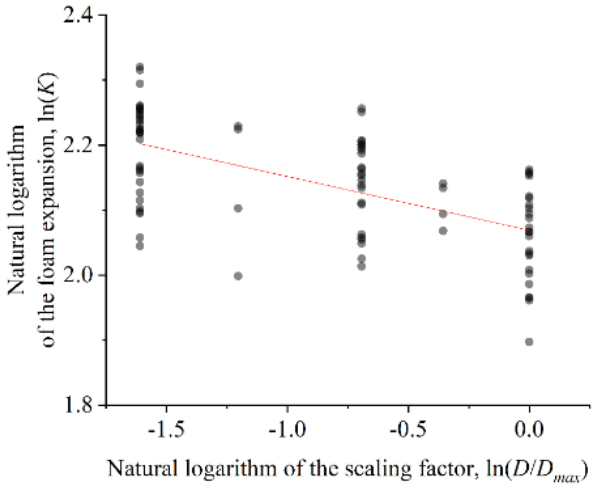

Figure 7. Dependence of the natural logarithms of the foam expansion and the outer deflector diameter of the sprinkler reduced to its largest diameter.

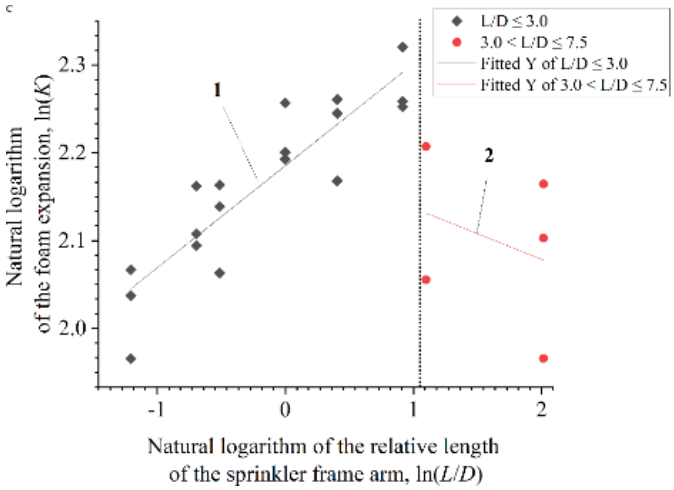

Figure 8. Dependence of the natural logarithms of the foam expansion and the relative length of the sprinkler frame arm (the slope of the fitted curves 1 and 2 are 0.10 and –0.03, respectively).

Five full factorial experiments were carried out to determine the dependence of the foam expansion on the Weber number. During experiments, five sprinklers with different dimensions of the nozzle flow path were used to change the character of the fluid flow. The design of the full factorial experiments included p = 4 factors $\left(L,\ K_s,\ D,\ \alpha\right)$ that varied on n = 3 value levels (since the dependencies of foam expansion on each factor are nonlinear as follows from [11]). Each full factorial experiment consisted of 81 series of experiments ($N = p^n = 3^4 = 81$). The design of full factorial experiments was similar to that described in detail in [11]. Fig. 9 shows the appearance and dimensions of the flow path of the sprinkler nozzle. The values of the Weber number at the orifice of the nozzle are also indicated. The operating pressure of the working foam solution with the manufacturer's recommended concentration of the foam concentrate before the sprinkler nozzle was 0.1 MPa and remained constant.

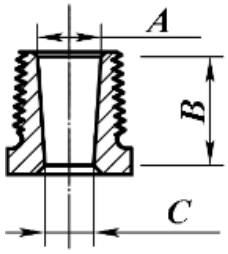

Nozzle	*A*, mm	*B*, mm	*C*, mm	*We*
No.1	12.3	20.9	9.5	$75 \cdot 10^3$
No.2	13.2	21.0	11.0	$68 \cdot 10^3$
No.3	20.0	22.0	13.5	$46 \cdot 10^3$
No.4	17.5	19.5	15.7	$37 \cdot 10^3$
No.5	20.0	24.5	17.6	$22 \cdot 10^3$

Figure 9. Appearance and dimensions of the flow path of the sprinkler nozzles (A is the diameter of the nozzle inlet; B is the length of the nozzle flow path; C is the diameter of the nozzle orifice; We is the Weber number at the nozzle orifice at operating pressure 0.1 MPa).

Fig. 10 shows the dependences of the natural logarithm of the foam expansion and the natural logarithm of the Weber number for 5 different configurations of the frame arm and deflector of the sprinkler (for the remaining 76 configurations, the character of the dependences is similar). Taking into account that in the studied range of changing the distance from the orifice of the nozzle to the deflector of the sprinkler (from 30 to 150 mm) the average jet velocity remains almost constant [29, 30], the Weber number was calculated for the liquid jet at the orifice of the sprinkler nozzle. Based on the obtained results, the average slope of the regression line of the dependence $\mathrm{In}\left(K\right) = f\left(\mathrm{In}\left(We\right)\right)$ is equal to z = 0.32. It should be emphasized that the Weber number growth causes an increase in the foam expansion as observed in Fig. 10. It can be explained by the growth of hydrodynamic pressure on the frame arm and deflector of the sprinkler that adds to the process of formation of a new surface and, accordingly, increases the number of forming foam films and bubbles.

The new simplified mathematical model (4) predictions of foam expansion show good agreement with the experimentally measured foam expansion. There was an average error in foam expansion of less than 9 % and the largest error of less than 20 % for all cases when the empirical coefficient Be = 0.026 was used.

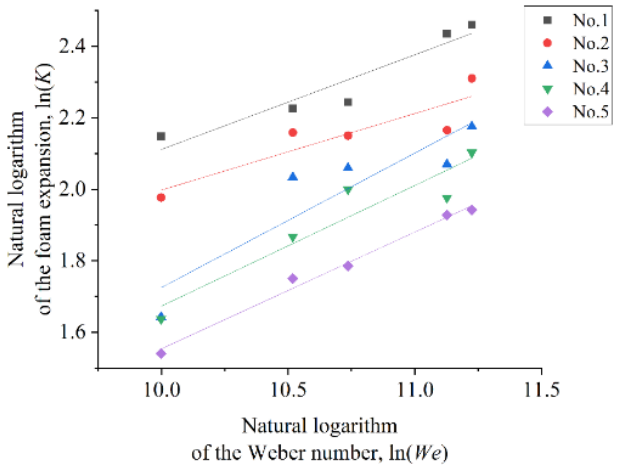

Figure 10. Dependence of the natural logarithms of the foam expansion and the Weber number with fitted curves (configurations of the frame arm and deflector geometric parameters: No. 1 – K_s = 87%, L = 114 mm, D = 63 mm; No. 2 – K_s = 100%, L = 50 mm, D = 20 mm; No. 3 – K_s = 55%, L = 50 mm, D = 50 mm; No. 4 – K_s = 64%, L = 100 mm, D = 30 mm; No. 5 – K_s = 64%, L = 30 mm, D = 100 mm).

Thus, the final form of the empirical equation for determining the foam expansion is as follows:

$$K = 0.026\gamma_{e.r}K_s^{0.5}\left(L/D\right)^{g}\left(D/D_{\max}\right)^{-0.05}We^{0.32}, \quad (5)$$

where $\gamma_{e.r}$ is equal to 1 for the foam concentrate PO-6RZ, 0.92 for Syntec-6NS and 0.68 for OPS-0.4; g is equal to 0.10 at L/D ≤ 3.0 and –0.03 at 3.0 < L/D ≤ 7.5.

The boundary conditions of the developed model (4) are as follows: K_s is from 55 to 100 %, L is from 30 to 150 mm, D is from 20 to 100 mm, We is from 22·10³ to 75·10³, $D_{\max}$ is equal to 100.

4. Conclusions

A novel simplified mathematical model (5) for predicting expansion of foam generated in the deflector type sprinklers in automatic foam extinguishing systems was developed. The predictions of this new foam expansion model are in good agreement with the experimentally measured values. The average foam expansion error was less than 9 %.

The developed model can be used as an express method to predict the foam expansion in sprinklers taking into account the dimensions of the frame arm and deflector of the sprinkler, jet hydrodynamics and the properties of the applied foam concentrate of type S or WA. If the applied foam concentrate differs from those mentioned in this article, the corresponding coefficient $\gamma_{e.r}$ must be substituted into the model (5). The coefficient $\gamma_{e.r}$ can be determined experimentally according to the method described in details in [27].

Further studies will be devoted to establish the physical nature and the dependence of the coefficient $\gamma_{e.r}$ on the physical properties of the foam concentrate, as well as its chemical composition. It will provide a way to make the developed model (5) applicable for any foam concentrate. In addition, at the moment, the dependence of foam expansion on other dimensionless parameters, for example, on the ratio of the parameters K_s (the deflector working surface coefficient) and L (the frame arm length), are poorly understood. This dimensionless parameter is likely to have a high correlation with foam expansion and may be fundamentally important. In addition, in future studies, solutions of single surfactants that are generally used to prepare foaming solutions for extinguishing fires (for example, an aqueous solution of sodium lauryl sulfate or similar commonly used surfactant) will be taken as a reference foaming agent. This will make it possible to increase the reproducibility of the results by other authors.

Moreover, further research should focus on developing models to predict two other very important characteristics of the foam in terms of firefighting, such as its dispersion and stability. Dispersion is a value inverse to the average diameter of bubbles in the foam volume, and stability is a value defined as the time of destruction of a certain part of foam volume. The ability to predict the main characteristics of the foam

will make it possible to evaluate more objectively the level of fire protection of buildings and structures by automatic foam extinguishing systems.

References

1. Chen, T., Fu, X.-C., Bao, Z.-M., Xia, J.-J., Wang, R.-J. Experimental study on the extinguishing efficiency of compressed air foam sprinkler system on oil pool fire. Procedia Engineering. 2018. 211. Pp. 94–103. DOI: 10.1016/j.proeng.2017.12.142
2. Shafiq, I., Hussain, M., Shafique, S. et al. A comprehensive numerical design of firefighting systems for onshore petroleum installations. Korean Journal of Chemical Engineering. 2021. 38. Pp. 1768–1780. DOI: 10.1007/s11814-021-0820-6
3. Till, R.C., Coon, J.W. Foam Systems. Fire Protection. Springer. Cham, 2019. Pp. 147–157. DOI: 10.1007/978-3-319-90844-1_11
4. Dlugogorski, B.Z., Kennedy, E.M., Schaefer, T.H., Vitali, J. What properties matter in fire-fighting foams? Proceedings of the 2nd National Research Institute of Fire and Disaster Symposium – Science, Technology and Standards for Fire Suppression Systems. Tokyo, 2002. Pp. 57–76.
5. International Organization for Standardization (ISO). Fire extinguishing media – Foam concentrates. Part 3: Specification for low-expansion foam concentrates for top application to water-miscible liquids. ISO 7203-3:2019. Geneva, 2019. 39 p.
6. Kamliuk, A.N., Likhomanov, A.O., Grachulin, A.V. Pennye orositeli dlia avtomaticheskikh ustanovok pozharotusheniia [Foam sprinklers for automatic extinguishing systems]. Minsk: UGZ, 2023. 244 p.
7. Korol'chenko, D.A., Sharovarnikov, A.F., Degaev, E.N. Fire extinguishing effectiveness of low multiplicity foam. Science Review. 2015. 8. Pp. 114–120.
8. Hil', E.I., Voevoda, S.S., Sharovarnikov, A.F., Makarova, I.P. Experimental determination of minimum discharge intensity and optimum rate of foaming agent input during suppression of oil products flame. Fire Safety. 2015. 4. Pp. 76–81.
9. Laundess, A.J., Rayson, M.S., Dlugogorski, B.Z., Kennedy, E.M. Small-Scale Test Protocol for Firefighting Foams DEF(AUST)5706: Effect of Bubble Size Distribution and Expansion Ratio. Fire Technology. 2011. 47. Pp. 149–162. DOI: 10.1007/s10694-009-0136-2
10. Myers, T.M., Marshall, A.W. A description of the initial fire sprinkler spray. Fire Safety Journal. 2016. 84. Pp. 1–7. DOI: 10.1016/j.firesaf.2016.05.004
11. Kamluk, A., Likhomanov, A. Increasing foam expansion rate by means of changing the sprinkler geometry. Fire Safety Journal. 2019. 109. Article no. 102862. DOI: 10.1016/j.firesaf.2019.102862
12. Kim, T. Resolving the initial spray structure of fire sprinklers with a volume-of-fluid modeling. Fire Safety Journal. 2016. 133. Article no. 103641. DOI: 10.1016/j.firesaf.2022.103641
13. Kim, T. Factors affecting water flux distribution of fire sprinklers and effect of water flux uniformity on fire suppression characteristics. Fire Safety Journal. 2023. 138. Article no. 103804. DOI: 10.1016/j.firesaf.2023.103804
14. Kim, T. Optimization of fire sprinkler design for uniform water flux distribution using a micro-genetic algorithm. Fire Safety Journal. 2024. 144. Article no. 104090. DOI: 10.1016/j.firesaf.2024.104090
15. Myers, T., Trouve, A., Marshall, A. Predicting sprinkler spray dispersion in FireFOAM. Fire Safety Journal. 2018. 100. Pp. 93–102. DOI: 10.1016/j.firesaf.2018.07.008
16. Myers, T., Marshall, A., Baum, H.R. A Free-Surface Model of a Jet Impinging On a Sprinkler Head. Fire Safety Science. 2014. 11. Pp. 1184–1195. DOI: 10.3801/IAFSS.FSS.11-1184
17. Link, E.D., Jordan, S.J., Myers, T.M., Sunderland, P.B., Marshall, A.W. Spray dispersion measurements of a sprinkler array. Proceedings of the Combustion Institute. 2017. 36(2). Pp. 3305–3311. DOI: 10.1016/j.proci.2016.06.056
18. Valencia, A., Marshall, A.W. A universal lookup table for determining sprinkler spray patterns. Fire Safety Journal. 2021.126. Article no. 103432. DOI: 10.1016/j.firesaf.2021.103432
19. Ren, N., Wang, Y. Modeling of Sprinkler skipping for the suppression of large-scale rack-storage fires. Fire Safety Journal. 2023. 141. Article no. 103953. DOI: 10.1016/j.firesaf.2023.103953
20. Kamluk, A., Likhomanov, A., Grachulin, A. Field testing and extinguishing efficiency comparison of the optimized for higher expansion rates deflector type sprinkler with other foam and foam-water sprinklers. Fire Safety Journal. 2020. 116. Article no. 103177. DOI: 10.1016/j.firesaf.2020.103177
21. Tafreshi, H.V., Pourdeyhimi, B. The effects of nozzle geometry on waterjet breakup at high Reynolds numbers. Experiments in Fluids. 2003. 35. Pp. 364–371. DOI: 10.1007/s00348-003-0685-y
22. Jie, H., Jingjing, W., Xiumei, L., Beibei, L., Wei, L., Ming, G., Yongwei, X., Zonghang, C., Jichao, M. Investigation on Surface Wave Characteristic of Water Jet. Mathematical Problems in Engineering. 2019. 2019. Article no. 4047956. DOI: 10.1155/2019/4047956
23. Lin, S.P., Reitz, R.D. Drop and spray formation from a liquid jet. Annual Review of Fluid Mechanics. 1998. 30. Pp. 85–105. DOI: 10.1146/annurev.fluid.30.1.85
24. Trettel, B. Reevaluating the jet breakup regime diagram. Atomization and Sprays. 2020. 30(7). Pp. 517–556. DOI: 10.1615/AtomizSpr.2020033171
25. Likhomanov, A.O., Kamlyuk, A.N. The breakup length of axisymmetric turbulent jet in the foam deflector type sprinkler for automatic extinguishing systems. Journal of Civil Protection. 2021. 5(2). Pp. 159–173. DOI: 10.33408/2519-237X.2021.5-2.159
26. Eggers, J., Villermaux, E. Physics of liquid jets. Reports on Progress in Physics. 2008. 71(3). Article no. 036601. DOI: 10.1088/0034-4885/71/3/036601
27. Likhomanov, A.O., Govor, E.G., Kamlyuk, A.N. On the relationship between the sprinkler geometric parameters, stability and expansion rate of the generated foam. Journal of Civil Protection. 2021. 5(2). Pp. 174-185. DOI: 10.33408/2519-237X.2021.5-2.174
28. Likhamanau, A., Kamluk, A. Mathematical model for predicting foam expansion rate depending on the geometrical parameters of deflector type sprinkler. Nauchnye i obrazovatelnye problemy grazhdanskoi zashchity [Scientific and educational problems of civil protection]. 2019. 41(2). Pp. 27–38.
29. Kotousov, L.S. Measurement of the water jet velocity at the outlet of nozzles with different profiles. Technical Physics. 2005. 50. Pp. 1112–1118. DOI: 10.1134/1.2051447

30. Kotousov, L.S. Measurement of the water jet velocity at the outlet of nozzles with different profiles. Technical Physics. 2006. 51. Pp. 289. DOI: 10.1134/S1063784206020265

Information about the authors:

***Andrei Kamluk**, PhD in Technical Sciences*
ORCID: https://orcid.org/0000-0002-9347-0778
E-mail: kan@ucp.by

***Alexey Likhomanov**, PhD in Technical Sciences*
ORCID: https://orcid.org/0000-0002-9374-1486
E-mail: alexlikh20@gmail.com

***Eduard Govor**,*
ORCID: https://orcid.org/0000-0002-4040-3264
E-mail: govor-098@mail.ru

***Alexander Grachulin**, PhD in Technical Sciences*
ORCID: https://orcid.org/0000-0003-3832-8258
E-mail: grachulin_a@mail.ru

Received: 09.07.2024. Approved: 13.10.2024. Accepted: 21.10.2024.